

Mediterranean drought fluctuation during the last 500 years based on tree-ring data

A. Nicault · S. Alleaume · S. Brewer · M. Carrer ·
P. Nola · J. Guiot

Received: 16 October 2007 / Accepted: 27 November 2007 / Published online: 15 January 2008
© Springer-Verlag 2008

Abstract A $2.5 \times 2.5^\circ$ gridded summer (April–September) drought reconstruction over the larger Mediterranean land area ($32.5^\circ/47.5^\circ\text{N}$, $10^\circ\text{W}/50^\circ\text{E}$; 152 grid points) is described, based on a network of 165 tree-ring series. The drought index used is the self-calibrated Palmer Drought Severity Index, and the period considered is 1500–2000. The reconstruction technique combines an analogue technique for the estimation of missing tree-ring

data with an artificial neural network for optimal non-linear calibration, including a bootstrap error assessment. Tests were carried out on the various sources of error in the reconstructions. Errors related to the temporal variations of the number of proxies were tested by comparing four reconstructions calibrated with four different sized regressor datasets, representing the decrease in the number of available proxies over time. Errors related to the heterogeneous spatial density of predictors were tested using pseudo-proxies, provided by the global climate model ECHO-G. Finally the errors related to the imperfect climate signal recorded by tree-ring series were tested by adding white noise to the pseudo-proxies. Reconstructions pass standard cross-validation tests. Nevertheless tests using pseudo-proxies show that the reconstructions are less good in areas where proxies are rare, but that the average reconstruction curve is robust. Finally, the noise added to proxies, which is by definition a high frequency component, has a major effect on the low frequency signal, but not on the medium frequencies. The comparison of the low frequency trends of our mean reconstruction and the GCM simulation indicates that the detrending method used is able to preserve the long-term variations of reconstructed PDSI. The results also highlight similar multi-decadal PDSI variations in the central and western parts of the Mediterranean basin and less clear low frequency changes in the east. The sixteenth and the first part of the seventeenth centuries are characterized by marked dry episodes in the west similar to those observed in the end of the twentieth century. In contrast, the eighteenth and nineteenth centuries (Little Ice Age) are characterized by dominant wet periods. In the eastern part of the Mediterranean basin the observed strong drought period of the end of the twentieth century seems to be the strongest of the last 500 years.

A. Nicault · S. Brewer · J. Guiot
CEREGE, UMR 6635 CNRS/Université Paul Cézanne,
BP 80, 13545 Aix-en-Provence Cedex 4, France
e-mail: brewer@cerege.fr

J. Guiot
e-mail: guiot@cerege.fr

A. Nicault (✉)
I.N.R.S., Centre ETE, 490 de la couronne,
Québec, QC G1K 9A9, Canada
e-mail: antoine.nicault@ete.inrs.ca

S. Alleaume
Cemagref, 3275 Route Cézanne,
13182 Aix en Provence Cedex 5, Germany
e-mail: alleaume@aix.cemagref.fr

M. Carrer
Dip. TeSAF - Treeline Ecology Research Unit - Agripolis,
Università degli Studi di Padova, 35020 Legnaro (PD), Italy
e-mail: marco.carrer@unipd.it

P. Nola
Dip. Ecologia del Territorio,
Università degli Studi di Pavia,
Via S. Epifanio 14, 27100 Pavia, Italy
e-mail: pnola@unipv.it

Keywords Climate reconstruction · Tree-ring · Mediterranean · PDSI · Drought

1 Introduction

Among the many reconstructions of temperature at global or hemispheric scales (Bradley and Jones 1993; Overpeck et al. 1997; Jones et al. 1998; Mann et al. 1998, 1999; Crowley and Lowery 2000; Briffa et al. 1998, 2001, 2002, 2004; Esper et al. 2002, 2004, 2005; Cook et al. 2004; Huang 2004; Pollack and Smerdon 2004; Moberg et al. 2005; D'Arrigo et al. 2006a, b; Osborn and Briffa 2006; Jansen et al. 2007) the large increase in temperatures at the end of the twentieth century is a common feature. However, the observed change is not homogeneous across the hemisphere and significant differences may occur between regions and seasons (Luterbacher et al. 2004; Guiot et al. 2005; Brazdil et al. 2005; Casty et al. 2005a; Xoplaki et al. 2005). Studies of past climate trends and changes within these regions could therefore help to understand climate variability at smaller spatial scales. Further, some regions are potentially more sensitive to climate change, for example the Mediterranean basin where general circulation models predict a significant warming and decrease in precipitation (Gibelin and Deque 2003; Hertig and Jacobeit 2007; Giorgi and Lionello 2007). Giorgi (2006) identified the Mediterranean basin as the most prominent hot spot of climate change in the world with a decline in precipitation of over 20% in period between April and September. Further, extreme climatic events are expected to become more frequent and intense in this region (Meehl and Tebaldi 2004; Rambal and Debussche 1995; Stott et al. 2004). The probability of exceptional warm periods, similar to the record summer of 2003, has increased in this region (Luterbacher et al. 2004; Stott et al. 2004; Büntgen et al. 2005; Xoplaki et al. 2006).

The complexity of the Mediterranean climate may result in quite different spatial responses to global change, and some authors have shown large differences between eastern and western Mediterranean for both winter precipitation and summer temperature (Xoplaki et al. 2003, 2004; Dunkeloh and Jacobeit 2003). Global changes may have a significant effect on this region, particularly for water availability. The region is currently characterised by a summer drought period, particularly in the south and southeast part of the Mediterranean basin, which, coupled with anthropogenic impact, has increased desertification (Le Houerou 1992; Greco et al. 2005; Esper et al. 2007). Future changes could have a highly negative impact on water resources and therefore important socio-economic implications.

In order to improve our knowledge of natural climate variability and explore the possible roles of various causal factors (greenhouse gases, volcanism, solar activity...)

scientists need sufficiently long data series from periods during which these forcings differed from today. Instrumental data are not available over a sufficiently long period to investigate whether these forcings have played an important role alone or in combination in climatic changes. We therefore need to extend these data by using proxy data (Bradley 1999). The most widespread and continuous proxies for this period are tree rings, especially in the Mediterranean region. Whilst documentary documents are also widespread in the Mediterranean region, they are often discontinuous and their quality decreases back in time (Luterbacher et al. 2006 and references therein). In contrast, the Mediterranean area offers a broad spectrum of dendroclimatological time series, both in time and space, making this area ideal for climate reconstructions prior to the instrumental period.

Previous studies on past Mediterranean climate are available for several regions, e.g. the Iberian Peninsula (Barriendos and Rodrigo 2005), southern Spain (Rodrigo et al. 1999, 2001), northwestern Spain (Saz 2004), southeastern Mediterranean (Touchan et al. 2003, 2005), the Alpine region (Casty et al. 2005) Sicily (Diodato 2007), Morocco (Esper et al. 2007; Till and Guiot 1990), southern Jordan (Touchan et al. 1999), central Turkey (D'Arrigo and Cullen 2001; Akkemik and Aras 2005), and the western Black Sea region of Turkey (Akkemik et al. 2005, 2007). A recent overview is given by Luterbacher et al. (2006). Briffa et al. (2001), and Guiot et al. (2005) have provided temperatures reconstructions for southeastern France and Spain. Other studies include flood (Llasat et al. 2003; Guibert 1994) or drought reconstruction (Barriendos and Llasat 2003; Piervitali and Colacino 2001; Esper et al. 2007). To date, the only temporally and spatially high-resolution reconstruction of precipitation for the Mediterranean basin has been developed by Pauling et al. (2006).

As Mediterranean droughts are linked to both a lack of precipitation and high evaporation, it is important to use an index, which takes into account the soil water availability for the vegetation rather than purely climatic variables. We have therefore chosen to reconstruct the Palmer Drought Severity Index (PDSI; Palmer 1965), which has been used in a number of previous tree-ring based studies, notably in the US (Cook and Jacoby 1977; Cook et al. 1988, 1992, 1999, 2004; Stockton and Meko 1983; Stahle and Hehr 1985; Stahle and Cleaveland 1988; Meko et al. 1993) but also in other countries (D'Arrigo et al. 2006a, b; Li et al. 2006; Esper et al. 2007). Van der Schrier et al. (2006, 2007) have estimated changes in summer moisture across Europe and Alpine region during the period 1801–2003. This index uses a rough estimation of the water contained in the soil, based on a running water balance calculation (soil water content from previous month plus the inputs and less the outputs) and therefore represents the water

available for vegetation. Verification tests show that PDSI reconstructions are reliable. Whilst previous reconstructions of temperature or precipitation gave significant and coherent results at a local scale, attempts to reconstruct large-scale temperature and precipitation from only tree-rings on this region were unsuccessful (the reconstructions did not pass any verification test). However, multiproxies reconstructions (Pauling et al. 2006) or, as shown here, PDSI reconstructions give much better results. PDSI success may be explained by three factors. (1) It integrates both temperature and precipitation that both influence the growth of vegetation to a varying degree. (2) It is a better estimator of water availability, which is the main climate-forcing factor in Mediterranean tree-physiology, than precipitation. (3) It has a memory component: the index for any given month is influenced by the amount of water fallen in the previous months. This results in an autocorrelation between the successive annual indices of a similar magnitude to tree-ring series autocorrelation.

There are several potential sources of uncertainty for this kind of reconstruction. For example, is the network of available proxy indicators dense enough for a meaningful estimation of regional climate? Can statistical models, calibrated with data at interannual timescales be used to estimate the low-frequency variability of the past climate? Zorita et al. (2003) have assessed these questions using the output from a long-term climate model simulation, and the reconstruction method proposed by Mann et al. (1998). The large-scale mean temperature of the model was reconstructed on the basis of different sets of selected model grid-points, representing the proxy indicators (pseudo-proxies). As expected, the results showed that there is a minimum number of proxy series required to reconstruct a significant part of the temperature variance. They also found that the low-frequency behaviour of the global temperature evolution is not always well reproduced. Another source of uncertainties has been tested by Von Storch et al. (2004), Burger et al. (2006) and Mann et al. (2005). Küttel et al.

(2007), where, in order to represent the imperfect relation between proxies and climate, the pseudo-proxies were degraded with statistical noise. We apply the same kind of tests here to evaluate the reliability of our tree-ring data for PDSI reconstructions, and robustness of our reconstructions. These reconstructions will improve the knowledge of spatio-temporal variability of drought in the Mediterranean basin, and place recent changes in an historical context. Further, these reconstructions allow climate models to be tested in a drought sensitive region.

2 Data

The study area is the Mediterranean region from 30°N to 50°N and from 10°W to 50°E. Three datasets are required for PDSI calculations: temperature, precipitation and local available water content (AWC) of the soil. Gridded precipitation and temperature data were extracted from the monthly $0.5 \times 0.5^\circ$ dataset compiled by the Climatic Research Unit TS 2.0 (Mitchell et al. 2004) (<http://www.cru.uea.ac.uk/cru/data/hrg.htm>), covering the period between 1901 and 2000. Soil available water capacity data were extracted from the ‘Global Soil Types, 1—Degree Grid’ (Zobler 1999). Calculation were made on $2.5^\circ \times 2.5^\circ$ degree grid, chosen as a trade-off between spatial resolution and a reduced number of grid points for data processing.

The tree-ring dataset comprised 136 sites distributed across the Mediterranean basin (Fig. 1), taken from the DENDRODB Relational European tree-ring database (<http://www.servpal.cerege.fr/webdbdendro/>).

In general in this region, tree growth occurs between April and September. Summer drought is the main limiting factor for most of the species growing under the Mediterranean climate. However, water available for growth is controlled by both summer and winter precipitation. Further, temperature influences evapotranspiration during this period. The signal is a complex combination of different

Fig. 1 Location of the 165 tree-rings series used in the reconstruction

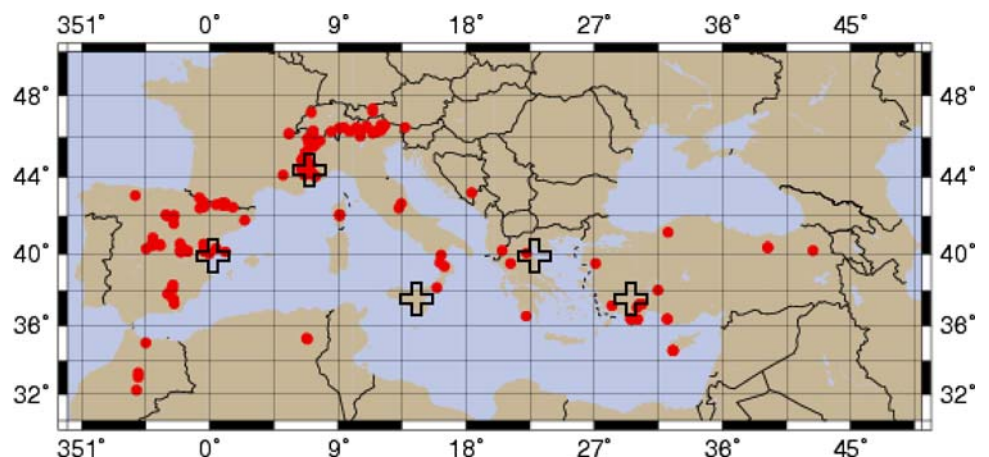


Table 1 Description of tree-ring series

Country	Ring-width series	Ring series	density	Species
Switzerland	2	2		<i>Picea abies</i> (3); <i>Larix deciduas</i> (1); <i>Pinus sylvestris</i> (1); <i>Pinus mugo</i> (1)
France	24	8		<i>Pinus cembra</i> (10); <i>Abies alba</i> (3); <i>Pinus sylvestris</i> (2); <i>Larix decidua</i> (8); <i>Picea abies</i> (2);
Italy	25	4		<i>Pinus cembra</i> (10); <i>Abies alba</i> (11); <i>Larix decidua</i> (10); <i>Picea abies</i> (8)
Spain	44	2		<i>Pinus sylvestris</i> (12); <i>Pinus nigra</i> (16); <i>Pinus mugo</i> (1); <i>Abies alba</i> (4); <i>Pinus uncinata</i> (11)
Morocco	5	0		<i>Cedrus atlantica</i>
Algeria	1	0		<i>Pinus halepensis</i>
Turkey	13	0		<i>Cedrus libanii</i> (2); <i>Pinus nigra</i> (2); <i>Pinus sylvestris</i> ; <i>Cedrus brevifolia</i> ; <i>Abies Nordmanniana</i> S.; <i>Juniperus</i> sp.
Greece	4	2		<i>Abies borisii</i> (2); <i>Abies cephalonica</i> (1); <i>Pinus nigra</i> (1)
Cyprus	4	4		<i>Pinus nigra</i> (3); <i>Cedrus brevifolia</i> (1);

climatic factors occurring during different periods. Summer drought is therefore a complex climatic parameter, and we use a set of different species from a wide variety of sites to obtain a better understanding of this complexity and to improve the spatial reconstitution. We have therefore retained all available series that are longer than 300 years (i.e. starting before 1700). The tree-ring measurements used in this study were the total ring width (RW), the final (or late) width (LW) and the maximum density (MD), as these are the most related to summer drought conditions. In total this gave 165 tree-ring series: 122 RW, 21 LW and 22 MD (Table 1).

3 Methodology

In summary, we first calculate the PDSI from instrumental data. Secondly, the tree-ring series are detrended. Thirdly, a transfer function is calibrated on the 1901–2000 period and then applied to tree-ring series up to 1350 AD. Finally, various tests are carried out to assess the reliability of the reconstructions.

3.1 PDSI calculations

The PDSI is based upon a set of empirical relationships derived by Palmer (1965) to represent the regional moisture supply, standardized in relation to local climatic conditions. A supply and demand model of soil moisture is used. The supply is the amount of moisture in the soil plus the amount that is absorbed into the soil from rainfall. The demand is more difficult to calculate, because the amount of water lost from the soil depends on several factors, including temperature and the amount of moisture in the

soil. A PDSI value is usually a combination of the current conditions and the previous PDSI value, so the PDSI also reflects the progression of trends, both droughts and wet spells. A modified version of the PDSI, the self-calibrated PDSI (Wells et al. 2004), was used for this study. In the self-calibrated PDSI, values for the duration factors and the climate characteristics are calculated for each location by examining the historical climate of the location.

The self-calibrated PDSI over the Mediterranean basin was calculated using the program developed by the National Agricultural Decision Support System (<http://www.nadss.unl.edu/PDSIReport/pdsi/>). We use the mean PDSI of the summer season (April–September), which is related to the water available during the growing season. The length of the season was chosen to cover the different growing periods of the species used, which could be very different according to tree-site geographical and altitudinal location. This growing season could be very short at high altitude (July–August) to very long at middle or low altitude (March–October). Growing season duration could also show strongly year to year change. PDSI integrates the seasonality of temperature and precipitation as it is a balance, month after month, between input and output water. So the choice of April to September growing season seems to be the best compromise between the geographically and species dependent growing seasons.

3.2 Standardisation of tree-ring data

Tree-ring series cannot be used directly as their long term variations are influenced by a number of non-climatic factors (Fritts 1976) that must be removed without distorting the climatic signal (Cook et al. 1995). There are many standard methods for detrending tree-ring series

(Fritts 1976; Cook et al. 1990). In many of these methods (negative exponential functions, regression functions, splines etc) individual series are detrended. This results in a loss of potential low frequency information. Over the last 10 years, there has been a shift to noisier methods that use a subset of ‘mean growth functions’ or ‘regional curves’ to capture lower frequency information. These methods are essentially the Regional Curve Standardisation (RCS) method (e.g. Briffa et al. 1992; Esper et al. 2004, 2007). Recent refinements of this method are detailed by Briffa et al. (2001) and Melvin (2004).

We have applied a RCS method, which has been shown to be the most appropriate method to preserve multicentennial climate variability (D’Arrigo et al. 2006a, b; Briffa et al. 1998; Esper et al. 2002; Melvin 2004). In order to minimize the bias due to differences in growth rate, the theoretical growth is considered as a function of age and productivity. This curve is then regionally calibrated with an Artificial Neural Network (Nicault et al. 2008), called the Adaptive Regional Growth Curve (ARGC). This method is based on the adaptation of the regional growth curve (RCS) to each tree, by taking into account the differences of mean productivity. Following Rathgeber et al. (1999), we postulate that the theoretical growth curve is a non-linear function of cambial age and tree productivity, which is a function of competition or soil. As the ARGC method takes into account, at least partially, differences in tree and site productivity observed during the juvenile growth period, it is able to minimise any bias introduced into the index series by differences in growth rates.

The tree-ring series are standardized into relative tree-ring indices by dividing each measured ring by its expected value estimated from a growth trend (Eq. 1). An artificial neural network (ANN) was used to estimate the growth curve trend for each tree from the cambial age, initial and maximum productivity tree (Eq. 2). We use a feed-forward network trained with the error back-propagation learning algorithm (Rumelhart et al. 1986). Productivity is taken into account on the basis of juvenile growth characteristics. Indexed series are obtained as follows (a script written in R is available from the authors):

$$I_t = \frac{C_t}{Y_t} \quad (1)$$

$$Y_t = F(\alpha(C_t), g(C), G(C)) \quad (2)$$

where

- Y_t is the theoretical value for tree-ring C_t ,
- $\alpha(C_t)$ is the age of tree-ring C_t ,
- $g(C)$ is the initial growth of tree C , i.e. the average of the first 10 rings,
- $G(C)$ is the maximal juvenile growth of tree C ,

i.e. the maximum value reached during its juvenile stage (first 50 years) after smoothing using a 10-year window.

These last two parameters (10 and 50 years) are chosen by the user and depend on the maximum age of the populations. For any given species in a given area the original RCS curve is built with all the populations available in the database (DENDRODB see above) for a given area, and not only those selected for reconstruction, in order to cover the maximum variety of ecological conditions and tree-age classes. RCS regions are defined according to relatively homogeneous climate features and population density. At least 50 trees had to be available to process the standardisation for a given area. For example three areas have been defined for *Pinus cembra* in Italian Alps: West, East and Center.

3.3 Climate reconstruction

The PDSI was reconstructed on a $2.5 \times 2.5^\circ$ grid covering the whole Mediterranean region ($32.5^\circ/50^\circ\text{N}$ $10^\circ\text{W}/50^\circ\text{E}$), for the period 1350–2000, with a full calibration period from 1901 to 2000. The technique used involves a combination of an analogue technique, to estimate missing data, coupled to an artificial neural network technique (referred to here as a transfer function) for optimal non-linear calibration (Guiot et al. 2005), and a bootstrap technique for calculating the error bars of the reconstruction. We have chosen to fill the matrix of proxies so that only a single transfer function is required. Other authors (Mann et al. 1998, 1999; Luterbacher et al. 2002, 2004; Xoplaki et al. 2005; Casty et al. 2005; Pauling et al. 2006) use a number of regressions based on a decreasing number of proxies. This is more time-consuming, and does not avoid the problem of missing values within proxy series.

Missing values in the predictor dataset is a problem, which has been solved in different ways. One is the nested regression: a regression is calibrated for each different subset of available predictors. This heavy procedure often leads to reconstructions with a variance decreasing with the number of really included predictors (Pauling et al. 2006). An alternative more and more frequently used is the regularized expectation maximization (REGEM), which impute missing values in a manner that makes optimal use of spatial and temporal information in the dataset (Rutherford et al. 2005). We propose another method, which has not this weakness as the number of predictors is maintained constant in time, using an analogue technique. In order to replace a missing year for any given tree ring series, we compared the existing data with all other series using a Euclidian distance. The corresponding year from

the eight nearest series (analogues) are averaged with a weight inversely proportional to the distance, to give a value obtained that is used to complete the missing tree-ring value. It should be noted that some missing values may remain, if too many missing values occur, or if no good analogues could be found. Results will show below that the reconstructed variance is well maintained independent on the number of predictors. The price to pay is the difficulty to quantify the total uncertainty on the reconstructions. Various validations of the results help to control this point (Sect. 2.4).

Standardized and completed tree-ring series were reduced using a principal component analysis (PCA) in order to remove the correlation between the regressors and to reduce their number. A PCA was also applied to the PDSI series in order to reduce the number of predictands, and to obtain a small number of synthetic variables representing the large-scale variations. The selected tree-ring series principal components (34) were then related to the selected PDSI components (24) using the same ANN technique described above. The summer PDSI during the last 650 years was then estimated by applying the transposed eigenvector matrix to the reconstructed principal components.

Cross-validation was used to assess the reliability of the extrapolation outside of the calibration period. The calibration interval was divided into two parts (1901–1950 and 1951–2000), we then (1) calibrated using the first part and verified on the second one, (2) calibrated using the second part and verified on the first, and (3) calibrated using the total dataset.

Errors from the ANN were assessed using a bootstrap method (Efron 1979). A subset of the observed data was randomly extracted with replacement. The ANN was then calibrated on this dataset and replicated 50 times, and each of the 34 predictand PC's were reconstructed separately. At each calibration, a determination coefficient between estimated and observed values was calculated for the data randomly taken for the calibration (the calibration R -squared, R_c^2), and another was calculated for the remaining data (the verification R -squared, R_v^2). Runs with a $R_c^2 < 0.20$ or a $R_v^2 < 0$ were rejected and any PC for which less than 10 runs were kept were rejected. The confidence interval for the reconstruction is given by the 5th and 95th percentile of the 50 reconstructions and corrected by the residual variance (Guiot et al. 2005). Additional statistics are also calculated at this step: the root mean squared error of the calibration data (RMSE), the root mean squared error of prediction of the verification data (RMSEP) and RE (Cook et al. 1994). As we use principal components instead of individual gridpoints, these statistics are regionally averaged for the whole Mediterranean reconstruction.

3.4 Tests for systematic errors in the reconstruction

The RMSE statistic tests the quality of fit on the calibration data, while the RMSEP and RE test the prediction capacity of the transfer function by using independent data. However, some additional error sources must be assessed and we examine here error due to (1) the variation in the number of predictors in time (in particular the low number of tree-ring series prior to 1500 AD); (2) the irregularity of the spatial coverage (in some regions, very few data are available); (3) the non-climatic noise included in tree-ring series.

3.4.1 Effect of the time-dependent number of proxies

In order to assess the impact of the decreasing number of available tree-ring series in earlier periods, three additional calibrations were made: one on the series that cover the period 1600–2000, i.e. 68 series; one for the series covering the period 1500–2000, i.e. 25 series; one for the series covering the period 1350–2000, i.e. 7 series. Including the full reconstruction, this resulted in four reconstructions that were then compared to assess the effect of the quantity of available information. In each case, despite the varying number of proxies, the analogue technique provides a quasi-full matrix for the total 1350–2000 period.

3.4.2 Effect of the space-dependent density of predictors

In the second test, we examined whether the statistical methodology remains valid in regions where the number of proxies is small. This concerns non-forested regions, e.g. Algeria (see map in Fig. 1), but also becomes much more widespread across the Mediterranean basin before 1500 AD as the number of available predictors drops below 10. To test the effect of the reduced number of proxies, we have used climate simulations of the global model ECHO-G (Legutke and Voss 1999) to represent both the proxies and target climate. This model consists of the spectral atmospheric model ECHAM4 coupled to the ocean model HOPE-G, both developed at the Max-Planck-Institut für Meteorology (Hamburg, Germany). The model ECHAM4 has a T30 horizontal resolution. The simulations used are driven by prescribed changes in volcanic forcing, solar irradiance, and greenhouse gases ('Erik-the-Red' simulation). We calculated self-calibrated summer PDSI using the method described above for instrumental data, based on monthly temperature and precipitation fields for the period 1350–1990.

Whilst simulations are available from another model HadCM3 (Gordon et al. 2000) for the same period, we have

chosen ECHO-G as it appears to be better correlated to our data (Brewer et al. 2006).

Each simulated proxy series (pseudo-proxy) is provided by the closest grid point to the tree-ring series. As the resolution of the model grid is much lower than that of the tree sites, the same pseudo-proxy may represent several predictors. The predictands, i.e. the climatic variables to be reconstructed are obtained by interpolation of the model grid to the $2.5^\circ \times 2.5^\circ$ instrumental grid. The method described in Sect. 2.3. is then applied to these two datasets., using the period 1901–1990 for calibration. As in Sect. 2.4.1, four calibrations are carried out, using the different predictor sets (165, 68, 25, 7) available for the four periods considered. An additional test is the examination of the spatial distribution of the correlations between observations and reconstructions, which are expected to be lower where less proxies are available.

3.4.3 Effect of the noise contained in the proxies

Calibration using a regression or other least-square method results in a loss of variance, which corresponds to the ratio between residual variance and predictand variance. A perfect regression (residual variance equal to zero) implies no loss, but usually the calibrated variance is between 50 and 80%, resulting in a loss of between 20 and 50%. This loss can have a significant impact on the low-frequency domain if the predictand (i.e. climate) has a red spectrum. In order to test this impact, we have used pseudo-proxies (von Storch et al. 2004; Küttel et al. 2007) described in Sect. 2.4.2, to which a varying proportion of statistical noise was added: $P_t^* = P_t + r\varepsilon_t S_P$ where P_t is a given proxy series (at time t), P_t^* is the noisy proxy, ε_t is a Gaussian random variable of mean 0 and variance 1, S_P is the standard deviation of proxy P and r is the ratio of noise that is added: $r = 0$ corresponds to a perfect pseudo-proxy without noise, $r = 0.5$ to a noise having half the standard deviation of the proxy, $r = 1, 2, 3, 4$ correspond to a noise having the same (double, triple, quadruple) standard deviation as the proxy. This test was carried out using the full dataset of the 165 proxy series available for the period 1700–1975.

The transfer function is calibrated for each dataset on the period 1901–1990 and applied to 165 pseudo-proxies back to 1350 AD. The various reconstructions are compared spatially as well as temporally.

4 Results

The first 34 principal components of the 165 indexed and filled (by the analogue technique) tree-ring series were

selected, explaining 82.3% of the total variance. The first 24 principal components of the 152 PDSI series were retained, explaining 89.9% of the total variance. The results presented here include the mean Summer PDSI calculated for the whole Mediterranean basin, and five representative gridpoints situated, respectively in Italy (37.5°N , 15°E), Turkey (37.5°N , 30°E), Spain (40°N , 0°E), Alps (45°N , 7.5°E) and Greece (40°N , 22.5°E). These points were chosen according the spatial distribution of the proxies (Fig. 1).

4.1 Effect of temporal and spatial decrease of proxies' number

4.1.1 Cross-validation test

The reconstructions using the two calibration subsets (1901–1950 and 1951–2000) were evaluated using the calibration correlation coefficients, the verification correlation coefficients, the correlation between the two reconstructions for the period 1350–2000 and the mean variance of each reconstruction for the same period, averaged for the whole basin (Table 2). The calibration for the period 1700–2000 with all the proxies available is excellent for both calibration sub-periods. More than 70% of the variance is reconstructed and the independent verification is also very good. Calibrations with subset of data corresponding to the periods 1600–1700 (1700-calibration), 1500–1600 (1600-calibration) and 1350–1500 (1500-calibration) remain highly significant even with a reduced number of proxies (Table 2). The correlation between the two reconstructions over the period 1350–1700 is very good for the 1700-calibration (165 proxies) and 1600-calibration (68 proxies) reconstructions, and although it decreases for the 1500-calibration (25 proxies), remains good. The variance calculated for reconstructions based on the 1700-, 1600- and 1500-calibrations (Table 2) varies between 0.5 and 0.8 but is much lower for the 1350-calibration (0.18–0.19). The RE calculated for each reconstruction (Table 2) based on the four calibrations datasets varies between 0.12 and 0.16 for the first calibration subset (1901–1950) and between 0.17 and 0.21 for the second subset (1950–2001), which means that the reconstructions are better than simply repeating the climatology through this period. The lower values observed for the reconstructions based on the 1350-calibration data set are still acceptable. Overall, and as expected, the correlations, the variance, and the RE of the reconstructed series decrease with the number of regressors used. However, with the exception of the reconstructed variance obtained using the 1350-calibration, the results are satisfying and cross-validation shows that correlations between

the PDSI reconstructions obtained from the two calibration subsets are still significant even when the number of proxies is low.

4.1.2 Comparison between ‘composite’ and ‘complete’ reconstruction

The analogue method has allowed the extension of all 165 tree-ring series back to 1350, but it is difficult to assess the quality of such extrapolations. We have therefore made a *composite* reconstruction (Meko 1997), constructed as follows: for the period 1700–2000, we have used the reconstruction based on all 165 series; for each earlier period (1600–1700, 1500–1600, 1350–1500), we have used the reconstruction obtained using only the proxies available for that period. This composite reconstruction has been compared to the reconstruction based on the maximum number of tree-ring series (the *complete* reconstruction) at the five selected grid points described above, for each of the earlier periods (Fig. 2).

The two curves are quite different during the period 1600–1700 periods, but remain very similar in variability and value. Correlations calculated on each sub-period show that whilst the correlations are good for the period 1600–1700 (0.22–0.57) (Table 3), the correlations decrease before 1600. Correlations are weak before 1600, but low frequencies are coherent. The poor correlation is explained by the reduced variability of the reconstruction obtained from the sub-period calibration.

A visual inspection of the curves (Fig. 2) shows that the differences for the 1500–1600 period still acceptable, with the exception of the Alps during the period 1500–1550. Prior to 1500, however, the differences become much larger, and the variance of the composite curves is too low (Table 4). During all periods, the variance of the complete reconstruction is always higher than the composite variance (Table 4), and both types of variance decrease with the number of predictors involved.

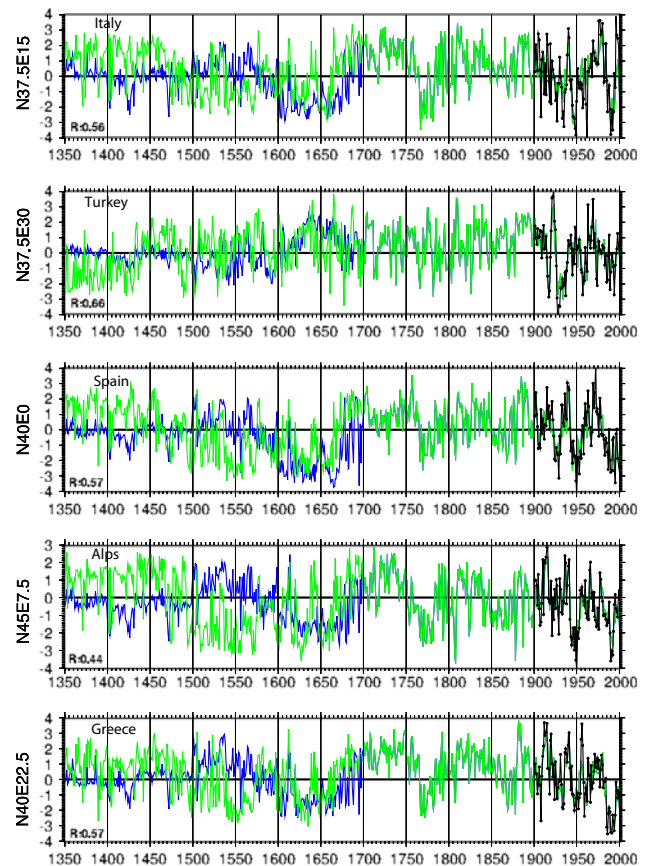


Fig. 2 Comparison of composites and complete reconstructions for each selected point: Italy (37.5°N, 15°E), Turkey (37.5°N, 30°E), Spain (40°N, 0°E), Alps (45°N, 7.5°E) and Greece (40°N, 22.5°E). In blue: composite reconstruction; in green PDSI complete reconstruction; in red: actual PDSI series

As the composite curves have much lower variability prior to 1500, we have chosen to use the complete series for further analysis. Further, we have rejected the reconstructions for the period 1350–1500, as we unable to test the quality of the replacement by the analogue method (the complete reconstruction). The following tests will then be done on the complete calibration and reconstruction from 1500 onward.

Table 2 Results of the test of cross validation for the two sub-periods 1901–1950, 1951–2000

	PC nb.	1901–1950 <i>r</i> calib	1951–2000 <i>r</i> verif	RE	1951–2000 <i>r</i> calib	1901–1950 <i>r</i> verif	RE	(Rec1 Rec2) <i>r</i>	Rec1 VAR	Rec2 VAR
1700–2000	34	0.84	0.78	0.16	0.88	0.89	0.21	0.72	0.33	0.53
1600–1700	23	0.88	0.73	0.13	0.83	0.88	0.23	0.77	0.65	0.87
1500–1600	17	0.86	0.76	0.11	0.76	0.63	0.21	0.54	0.60	0.80
1350–1500	6	0.76	0.62	0.12	0.68	0.83	0.17	0.85	0.19	0.18

The table shows the mean calibration multiple correlation coefficients, the mean verification multiple correlation coefficients, and the RE calculated for each sub period, the mean correlation between the two reconstructions on the 1350–2000 period (Rec1-Rec2 *r*) and the mean variance of each reconstruction on the 1350–2000 period (Rec1VAR, Rec2VAR), calculated for the whole Mediterranean basin

Table 3 Correlation coefficient between composite curve and complete curve calculated for the 1350–1500, 1500–1600, 1600–1700 sub-period on the 1350–1700 period, for each selected point

	1350–1500	1500–1600	1600–1700
Italy	0.02	−0.04	0.55
Greece	0.13	−0.16	0.57
Spain	0.05	0.20	0.54
Alps	0.06	−0.16	0.48
Turkey	0.06	0.33	0.22

Table 4 Variance of the composite and complete reconstructions for the 1350–1500, 1500–1600 and 1600–1700 periods, for each selected point

periode	Reconstruction	Italy	Greece	Spain	Alps	Turkey
1350–1500	Composite	0.50	0.33	0.27	0.31	0.13
	Complete	1.50	1.28	1.65	1.52	1.89
1500–1600	Composite	0.81	1.05	1.02	0.81	0.80
	Complete	1.47	2.02	1.76	1.31	1.59
1600–1700	Composite	1.73	1.41	2.08	1.25	0.92
	Complete	2.62	2.07	2.57	2.91	1.88

4.2 Bootstrapped PDSI reconstruction

The results of the reconstruction for each PDSI PC are shown in Table 5. For the first PDSI PC, which explains 22% of the PDSI variation in the Mediterranean basin, the tree-ring series explain 97.5% of the variance of this component with a 90% confidence interval of [0.92, 0.98]. The squared correlation for the verification is 0.90 with a 90% confidence interval of [0.57, 0.97]. The reconstruction remains highly significant for the first 14 PCs. The R_C^2 of the ten following components is statistically weak or non significant, and these have been rejected. The total variance explained can be calculated by combining the R^2 with the variance of each PC. The results are highly significant as 73% [62, 78] of the PDSI variance is explained with a R^2V of 0.49 [0.19, 0.63].

RMSE, RMSEP, and RE coefficients are mean values calculated for the whole reconstruction (Table 5), but RMSE is based only on the observations retained for the bootstrap calibration, whereas RMSEP and RE are based on the observations not used in the calibration (Table 5). The values obtained (RMSE: 0.92, RMSEP: 1.09, RE: 0.55) follow the good correlations values obtained with the bootstrap test and thus confirm the reliability of the reconstruction. When the calibration is made on a period of only 50 years, RE is positive but relatively low. However, when the calibration is made on a higher number of observations during the bootstrap procedure (2/3 of the

observations dispersed throughout the 1901–2000 period), the RE is much higher (0.55). This may be due to the fact that there is a trend in the twentieth century, which reduces the stationarity of the period.

Whilst the mean correlation coefficient is highly significant for the whole Mediterranean basin, the map of the correlations between observations and reconstructions across the 1901–2000 interval (Fig. 3) shows that there is a great deal of spatial variability in the amount of grid point PDSI variance explained by the proxy dataset, and the correlations are low (<0.75) in some southern regions. In Morocco, Spain, South-France, Italy, Greece, and Turkey, however, the PDSI variability appears to be well explained by the proxies. This corresponds roughly to the zones with the highest density of proxies.

The bootstrap reconstructions for the five selected grid points are shown in Fig. 4. The reconstructed PDSI for Turkey shows a number of differences from other regions. For example the humid period between 1660 and 1760 observed in the west has no equivalent in Turkey.

4.3 Test using GCM simulations as pseudo-proxies

4.3.1 Effect of spatial heterogeneity

The correlations between the pseudo-proxy based PDSI reconstructions and the target ECHO-G climate decrease from 0.92 with 34 PCs to 0.78 with 6 PCs (Table 6). In addition, the variance of the four reconstructions decreases as the number of predictors decreases, which is expected. Even the reconstruction based on the second highest number of pseudo-proxies (1700-reconstruction) shows a marked decrease in variance. Further, the errors bars associated to the five reconstructions increase when the number of available pseudo-proxies decreases (Fig. 5). This is expected, but what is less obvious is the fact that the reconstructions themselves are quite similar. Our method is then able, in theory, to reconstruct PDSI when the proxies have a very good quality, even if their number is low, and this has little effect on the error bars. The problem emerges when the proxies are noisy: this will be tested in the next section.

The spatial effect of the reduction in the number of pseudo-proxies is shown in Fig. 6. As the number decreases, the PDSI becomes increasingly poorly reconstructed in areas located at distance from the pseudo proxies. The averaged PDSI remains correctly reconstructed even when local reconstructions are poor. Maps of correlations, between observed PDSI and the four PDSI reconstructions, (Fig. 6) show that there is a great deal of spatial variability in the amount of grid point PDSI variance explained by the pseudo-proxy dataset, and the correlations are weak

Table 5 Statistical results of the bootstrapped ANN technique reconstruction, calibrated on the whole 1901–2000 period

Variable	%	5%_calib_R	50%_calib_R	95%_calib_R	5%_verif_R	50%_verif_R	95%_verif_R
PC 1	22.22	92.13	97.71	98.43	57.04	90.53	96.88
PC 2	12.4	74.87	86.78	93.51	18.08	60.27	72.84
PC 3	8.19	86.65	94.31	97.21	12.63	72.64	83.42
PC 4	7.66	63.57	88.56	93.93	11.3	52.22	74.96
PC 5	5.32	61.97	82.3	89.99	0.38	34.52	66.11
PC 6	4.36	73.6	82.37	87.82	10.31	45.27	70.35
PC 7	3.59	60.17	79.95	90.24	8.02	34.34	67.25
PC 8	3.36	66.74	78.15	86.44	5.74	42.27	64.4
PC 9	2.69	29.35	78.96	87.69	8.75	37.86	57.15
PC10	2.42	70.11	77.8	84.05	13.28	30.3	57.07
PC11	2.23	57.41	71.13	82.03	4.82	22.69	41.92
PC12	2.06	64.68	71.91	80.67	9.26	32.16	48.78
PC13	1.8	61.67	81.25	89.05	10.66	44.24	65.99
PC14	1.57	40.82	64.3	75.57	2.79	16.65	42.46
PC15	1.48	0	0	0	0	0	0
PC16	1.27	50.18	62.34	79.65	0.36	10.76	22.2
PC17	1.19	38.43	52.37	61.01	0.68	8.96	30.79
PC18	1.14	38.34	66.98	76.77	0.34	16.38	31.09
PC19	0.96	54.4	61.75	71.4	0.88	16.96	37.13
PC20	0.9	0	0	0	0	0	0
PC21	0.87	0	0	0	0	0	0
PC22	0.77	0	0	0	0	0	0
PC23	0.75	45.89	57.86	66.69	0.47	10.38	27.09
PC24	0.71	0	0	0	0	0	0
General		61.9	73.2	77.9	18.9	48.7	62.6

Mean R^2 with 90%-confidence interval calculated both on calibration and on verification datasets for each PC and for the general reconstruction including all the PC variance

(<0.75) in some southern regions. We can conclude from these maps that, from a strict methodological point of view, the number of predictors is sufficient almost everywhere after 1500. Prior to this period, the PDSI cannot be reconstructed for a number of large zones, even with perfect pseudo-proxies.

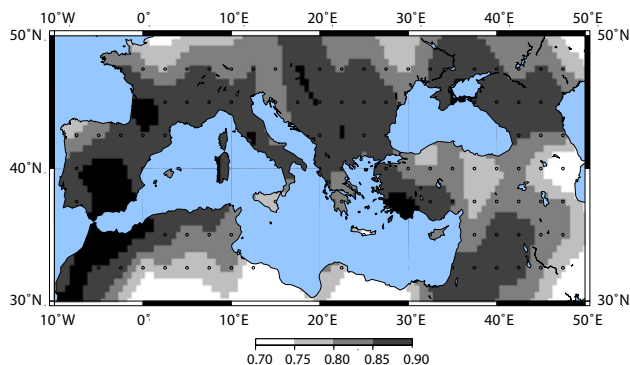


Fig. 3 Reconstruction of the summer PDSI with bootstrapped ANN method: spatial repartition of the R^2

4.3.2 Effect of the noise

When noise is added to the pseudo-proxies to represent the imperfect relation between proxies and climate, the correlations between the reconstructions and the target ECHO-G PDSI decrease as the noise increases (Table 7). Whilst the variance of the noisy reconstructions is always lower than that of the perfect curve, they remain highly significant. A closer examination shows that the all reconstructed PDSI series are flatter than the target ECHO-G series, indicating that the noise affects the low frequencies of the reconstructions (Fig. 7). These low frequencies are also systematically underestimated likely due to the fact that the calibration period is in mean drier than the extrapolation period. The medium frequencies remain well reconstructed, particularly for the period 1750–2000. The high correlations suggest that high frequencies are also well reconstructed. The main conclusion from this test is that noise, which is by definition a high frequency component, has a major effect on the low frequencies of the signal, but not on the medium or high frequencies.

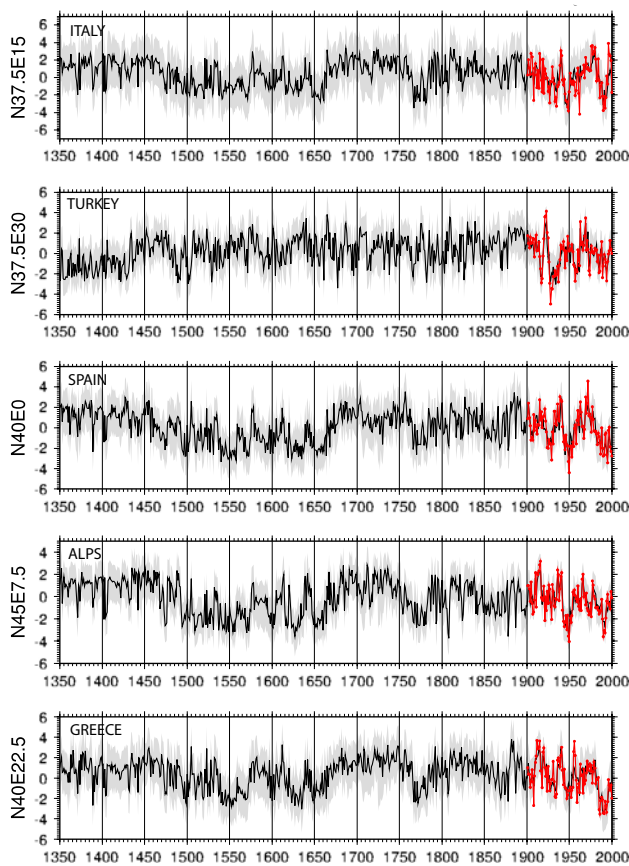


Fig. 4 Reconstruction of the summer PDSI with bootstrapped ANN method for the five selected point Italy (37.5°N, 15°E), Turkey (37.5°N, 30°E), Spain (40°N, 0°E), Alps (45°N, 7.5°E) and Greece (40°N, 22.5°E). *In red* actual PDSI series

5 Discussion

5.1 Reconstruction quality

The tests performed for the instrumental period show the reconstructions to be highly significant for the entire Mediterranean basin, at least during the twentieth century. We have used pseudo-proxies to assess the ability of the method to reconstruct PDSI during earlier periods and different regions of the study area.

Table 6 Results of the pseudo-proxy test

	PSPz_1700	PSPz_1600	PSPz_1500	PSPz_1350	ECHO_G
VAR	0.69	0.64	0.50	0.50	1.20
r (PSPrec, EchoG)	0.92	0.87	0.84	0.78	
r (TRrec, PDSI)	0.85	0.81	0.72	0.49	

Variance of each reconstruction of mean summer PDSI using pseudo-proxies (Calibrated with different sets of proxies for 1350, 1500, 1600, 1700), correlation coefficient between these reconstructions (PSPrec) and ‘perfect’ ECHO_G simulation and, as element of comparison, correlations between PDSI reconstructions from tree-ring data (TRrec) and Actual PDSI Data

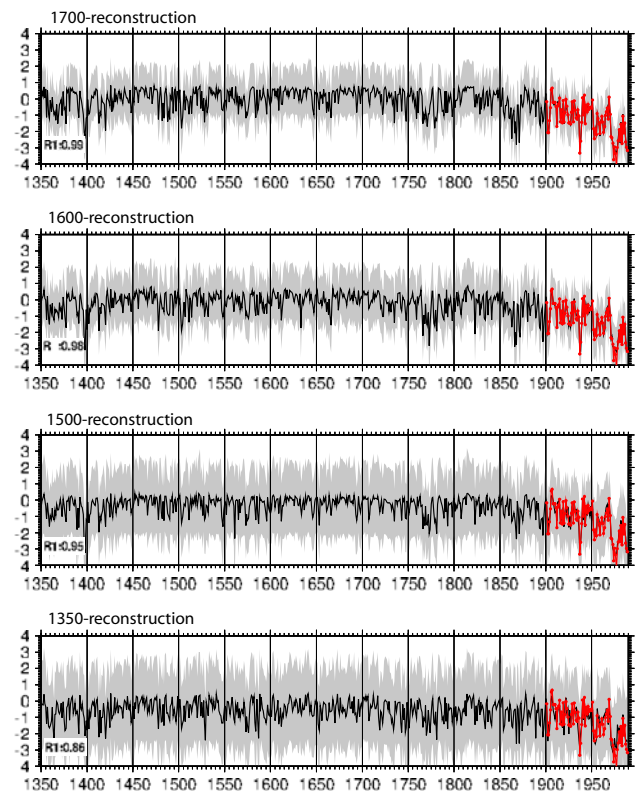


Fig. 5 Reconstruction of the mean summer PDSI (all Mediterranean area) based on a different number of pseudo-proxies: from 136 (top) to 7 (bottom)

The first pseudo-proxy based test confirms the results of Zorita et al. (2003), showing that the main effects of a reduction of the number of predictors are an increase in the error bars associated with the reconstruction and a decrease in the reconstruction variance. The averaged curve is, however, much more robust. The second test (Von Storch et al. 2004), shows that, whilst the variance of noisy reconstructions is always lower than the variance of the target curve, the high and intermediate frequencies are relatively well preserved with similar fluctuations observed in all curves. The white noise added to the pseudo-proxy series, which is by definition a high frequency component, has a major effect on the low frequencies of the signal.

Fig. 6 Reconstruction of the summer PDSI using pseudoproxies: correlation between simulated PDSI by ECHO-G-all at $2.5 \times 2.5^\circ$ gridpoints and their estimates using pseudo-proxies. *White points* indicate the position of the pseudo-proxies. The four graphics correspond to the four reconstructions implying each a different number of predictors for calibration (see text)

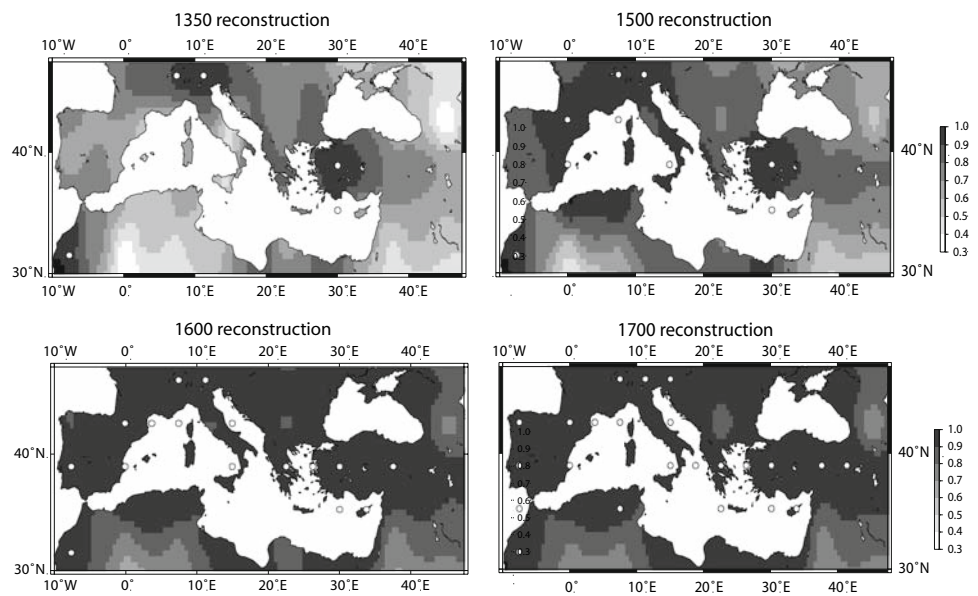


Table 7 Results of the noisy pseudo-proxies test

	PSPst0.5	PSPst1	PSPst2	PSPst3	ECHO_G
VAR	0.43	0.53	0.70	0.42	1.20
r (PSPs, ECHO)	0.86	0.82	0.67	0.73	

Variance of each reconstruction of mean summer PDSI using noisy pseudo-proxies (with a proportion of 0.5, 1, 2 and 3 of white noise variance) and correlation coefficient between these reconstructions and ‘perfect’ ECHO_G simulation

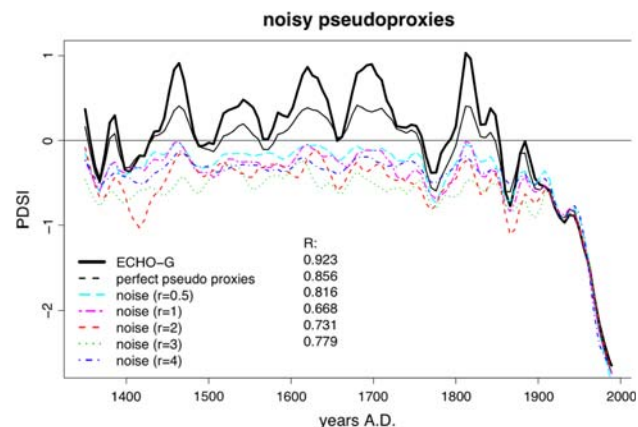


Fig. 7 Reconstruction of mean summer PDSI using noisy pseudo-proxies with a proportion of 0.5, 1, 2 and 3 of white noise variance compared to the mean ECHO-G simulation

Climatic reconstructions based on highly noisy proxies may therefore underestimate the long-term variations.

In addition, we have shown that the reconstruction for the period 1500–2000 is good or acceptable, but the reconstruction over 1350–1500 is not based on a sufficient

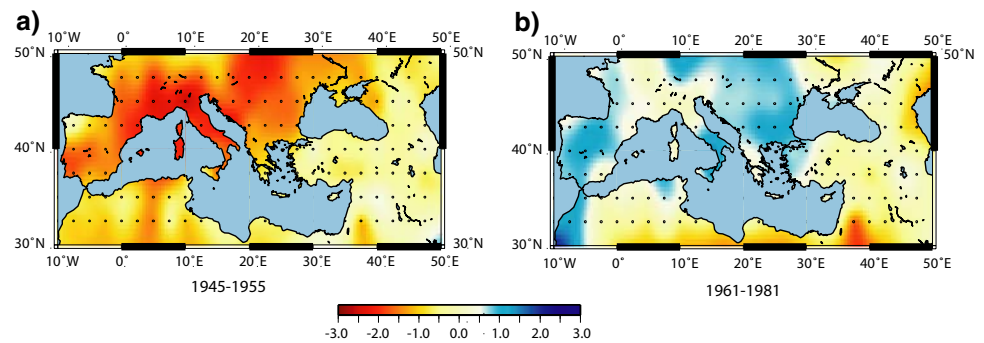
number of predictors for the low and intermediate frequencies to be considered as reliable. Comparison of spatial variation in the pseudo-proxy and tree-ring data reconstructions shows that low correlation coefficients, between actual and reconstructed values, are not linked with data quality but with the presence-absence of proxy data. The combination of these tests has allowed us to assess the reliability of tree-ring data set to reconstruct the PDSI, and thus to help in the interpretation of the results.

5.2 PDSI variations

PDSI is a combination of precipitation and temperature that takes into account the water soil capacity, giving it a climatic memory. The previous winter conditions will affect the value of PDSI in summer and even previous years could have an effect. It is therefore difficult to correlate this index directly with precipitation and/or temperature. However, the use of precipitation and temperature in the PDSI calculation allow an integration of these variables as effective droughts, which are the main characteristic of the Mediterranean climate. Dai et al. (2004) and Mika et al. (2004) have shown a good correlation of PDSI and soil moisture at global to local scales, and the ability of PDSI to well represent meteorological spatial variability.

Four of the five selected grid points (Spain, Alps, Italy, and Greece) show very similar long-term PDSI variations over the last 500 years (Fig. 4). Only the Turkish grid point shows different patterns. This confirms the dipole nature of the Mediterranean climate, with drier conditions over the western part and wetter condition over the eastern Mediterranean, previously shown by several authors (Kutiel

Fig. 8 Spatial pattern of PDSI over the Mediterranean basin for two period of the 20th century 1945–1955 (a); 1961–1981 (b)



et al. 1996a, b; Cullen and deMenocal 2000; Xoplaki 2002; Xoplaki et al. 2003, 2004, Pauling et al. 2006; Luterbacher et al. 2006). In terms of large-scale atmospheric circulation, this spatial pattern has been principally associated with the North Atlantic Oscillation (NAO), but also with an East Atlantic/Western Russia pattern (EAWRUS) (Xoplaki et al. 2003, 2004). The complex topography of Mediterranean basin with thermal and orographic forcing (Fernandez et al. 2003) also plays a role in this dipole (Xoplaki et al. 2003). In our reconstruction this well-marked dipole pattern is probably represented by the first principal component.

In the western and central Mediterranean basin, the twentieth century is characterized by variations between marked dry and wet periods, for example the dry period 1945–1955 (Fig. 8a) and the wet period 1961–1981 (Fig. 8b). In this region, twentieth century PDSI fluctuations are similar to the period of high variability between the second part of the sixteenth century and the first part of the seventeenth century. A marked decrease in PDSI values can be observed in the western part of Mediterranean (Spain and Morocco) during the last few decades of the twentieth century. The values, however, remain similar to the severe drought period of the sixteenth and seventeenth centuries. These periods of drought are coherent with Esper et al. (2007) drought reconstruction in Morocco, as the following wet period observed up to the twentieth century. In the eastern Mediterranean, the most important drought period occurred between 1925 and 1940 (Fig. 4). This drought is one of the harshest and longest observed during the last 500 years. This dry period was previously mentioned by Purgstall (1983) (in Touchan et al. 2005) who noticed a sustained famine during the 1925–1928 period, and by Touchan et al. 2005 who noticed the same 4 year drought period and the 1935 extreme drought period. Despite a less marked reduction in PDSI values over the last few decades in the eastern Mediterranean, the twentieth century is significantly the driest period of the whole Mediterranean region (mean PDSI = -0.10 with standard deviation of 0.13) of the last 500 years (mean PDSI of the 400 previous years = 0.55 with standard deviation 0.26).

5.3 The 1500–1650 period

This period was generally characterized by dry conditions (Fig. 4). The sixteenth and the first part of the seventeenth centuries are, in general, the driest period of last 500 years. The first part of the sixteenth century (1500–1540) shows a slight decrease of PDSI from wet (end of the fifteenth century) to severe dry conditions. The period from the middle of the sixteenth century to the middle of the seventeenth is characterised by alternating wet and dry periods. The drought periods are greater in intensity and duration than the wet periods. Three well-marked drought can be observed: 1540–1575 (Fig. 9a for the year 1540), 1620–1640 (Fig. 9c), and 1645–1665.

The generally dry conditions of this period and the large fluctuations in climate shown by our reconstruction are coherent with several previous studies of the LIA in Europe and the western Mediterranean area. The alternating warm and cold phases and wet and dry phases, reconstructed by Glaser et al. (1999), are coherent with the high PDSI variability. The year 1540 was the warmest and driest one in Europe (Glaser et al. 1999; Casty et al. 2005). Our results confirm that a severe drought occurred this year across the Mediterranean basin (Fig. 9a). Whilst no clear similarities can be seen between our reconstructions and the precipitation reconstructions for southern Spain (Rodrigo et al. 2000) and Morocco (Till et al. 1988), there is better correlation with other western Mediterranean zones. Saz (2004) have shown a significant opposition between annual mean temperature and total annual precipitation in Northern Spain. Low precipitation is related to high temperatures for the period 1540–1560 and around 1600, and with low PDSI. High precipitation is related to low temperatures around 1575 and around 1610, and to high PDSI. This underlines the interest of using the PDSI, which represents the opposition between temperature and precipitation rather than only precipitation variations. The reconstruction of a drought index by Barriendos and Llasat (2003) for Catalonia shows very similar pattern to our PDSI reconstructions during the period 1550–1650. The catastrophic flood event index, reconstructed by Llasat et al. (2005), and

the reconstruction of Durance river (Southern Alps) flood events (Guibert 1994) are also in agreement with our results, notably during the 1575–1620 period. In Sicily, Piervitali and Colacino (2001) observed that during the sixteenth and seventeenth centuries religious processions for rainfall were more frequent than during the eighteenth and nineteenth centuries, confirming our reconstructions for Southern Italy.

The high climatic variability of the sixteenth and seventeenth centuries in the western Mediterranean is not observed in the east, where no long drought or wet periods occurred. A marked dry period occurred around 1500, and has been shown in previous studies, including a reconstruction of March–June precipitation (Akkemik et al. 2005), April–August precipitation (Akkemik and Aras 2005) and May–August precipitation (Touchan et al. 2005). During several well-marked periods, the eastern Mediterranean is in opposition with the west, for example during 1540 to 1560 and 1620 to 1640 (Fig. 9c). These events seem to be analogous to the 1945–1950 period.

5.4 The 1650–1900 period

The Maunder Minimum (1645–1715) marks the transition from the dry conditions of the sixteenth and early seventeenth century, to the longest wet period (1670–1765). This transition (1665–1700) corresponds to the one of the coldest periods of the Little Ice Age (Pfister 1999; Jones et al. 1998; Briffa 2000; Luterbacher et al. 2000, 2001; Büntgen 2005). This long stable and wet period (1700–1750) affected the entire Mediterranean Basin with a relatively homogeneous pattern of high PDSI values (Fig. 9d). The only dry conditions are observed in the eastern part of Turkey. These observations are coherent with previous studies from the Mediterranean area (Rodrigo et al. 2000; Xoplaki et al. 2001; Barriendos 1997), which show that the climate, both in western and eastern Mediterranean, was colder and slightly wetter. These wet conditions were interrupted by a well-marked period of low PDSI values (1760–1780) (Fig. 9e). This period is comparable to the sixteenth to seventeenth century's drought period in intensity and in length. However the spatial pattern is somewhat different, with a clear opposition between a dry north and a normal to wet south. In the Alps, this period corresponds to a marked dry period, particularly after 1770 (Casty et al. 2005), which is associated with relatively high summer temperatures across Europe (Luterbacher et al. 2004). In Spain, Barriendos and Llasat (2003) have shown an increase in the drought index during this period and Creus et al. (1995) observed some anomalously dry springs.

The nineteenth century was dominated by wet conditions although with a relatively dry period around 1860. However, this century is mainly characterised by a highly variable PDSI values, with rapidly alternating wet and dry episodes and extreme values.

In southern Italy, the wettest year, 1810, follows the driest years in the Alps (1807–1808, Fig. 9f). These 2 years with very low PDSI values correspond to a succession of hot summers in France, and Casty et al. (2005) described 1807 as the warmest alpine summer. The PDSI pattern for these 2 years shows low to very low values for the whole Mediterranean basin. In the last few decades of the nineteenth century (Fig. 9g) the spatial pattern of PDSI values shows a well-marked opposition between northern part of the Mediterranean basin where dry conditions prevailed and the southern part where wet conditions prevailed. This period is characterised by a predominance of negative NAOI index, with an atmospheric situation causing increased rainfall in the Mediterranean region (Yiou and Nogaj 2004; Cullen et al. 2002; Luterbacher et al. 2006; Vinther et al. 2003), with the exception of 1882 (Fig. 9h), which is an extreme positive NAO. The existence of more frequent negative NAO atmospheric conditions during the eighteenth and nineteenth century (Luterbacher et al. 2002; Pauling et al. 2006), could explain the dominance of humid conditions.

6 Conclusion

This study is the first large scale PDSI reconstruction in the Mediterranean area. The index was reconstructed on a $2.5^\circ \times 2.5^\circ$ grid from tree-ring series covering the whole Mediterranean basin (10°W – 45°E and 30°N – 50°N) for the period 1350–2000. Several tests were used to assess the reliability of this reconstruction, including variations in the spatial and temporal densities of predictors. In particular, the use of pseudo-proxies provides a good method to examine the effect of problems in the method or dataset for periods where no instrumental data is available. The statistical significance of the reconstruction shows that tree-ring series provide well-adapted proxies for water availability in the Mediterranean region. The reconstruction shows well defined temporal and spatial variability of PDSI over the study area and time period. It shows, in particular, a very high PDSI variability during the sixteenth and seventeenth century (Early LIA), dominated by severe drought conditions, and a eighteenth century (maximum LIA) characterised by a stationary wet period notably during the first 60 years. The spatial patterns show frequent oppositions between the east and west of the region during the sixteenth to seventeenth centuries and between the north and the south during the eighteenth, nineteenth and twentieth centuries.

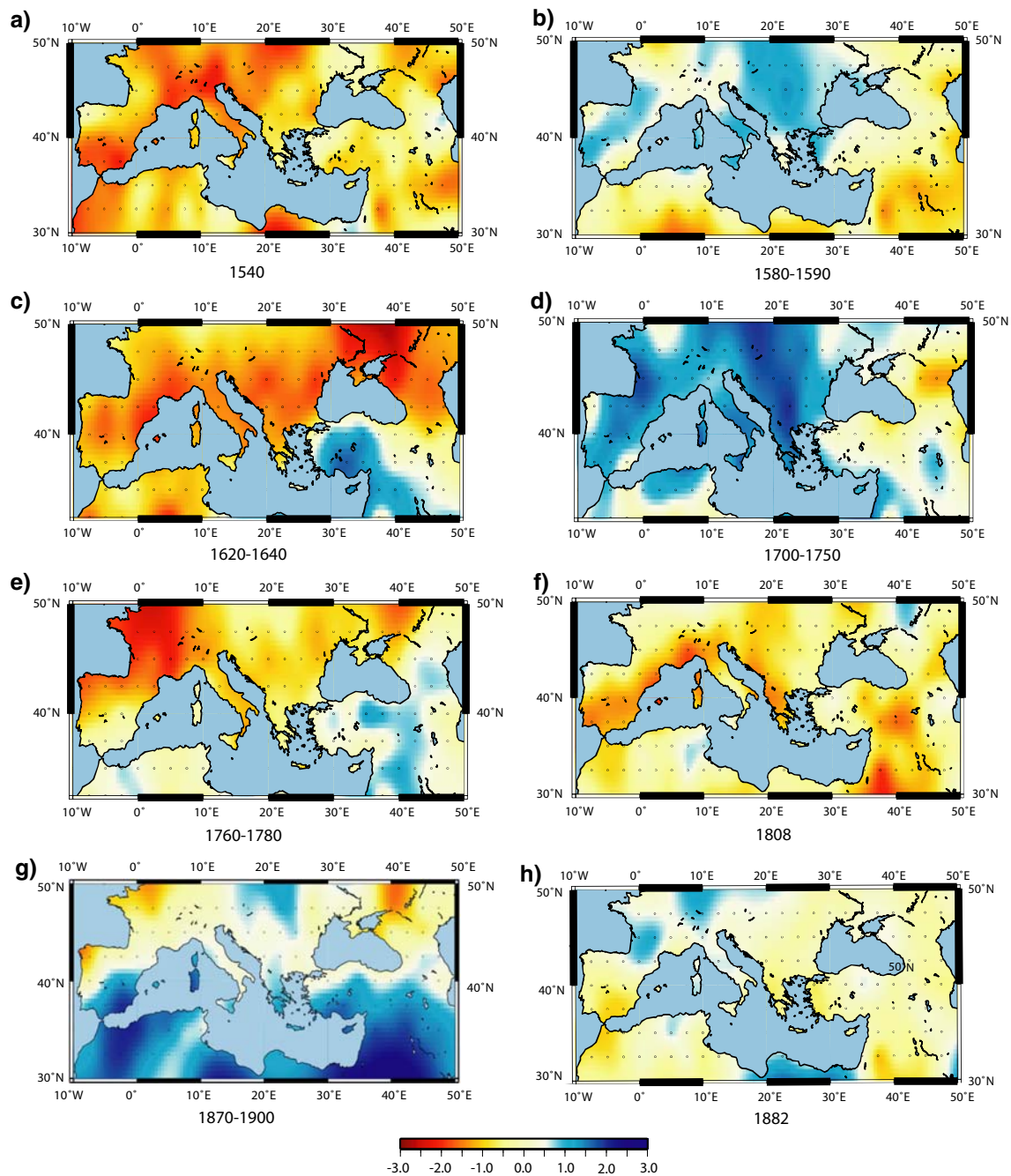


Fig. 9 Spatial pattern of PDSI over the Mediterranean basin for selected years [1540 (a); 1808 (f); 1882 (h)] or period [1580–1590 (b); 1620–1640(c), 1700–1750 (d); 1760–1780 (e); 1870–1900 (g)] over the last 500 years

During the twentieth century, the amplitude and duration of PDSI variations are similar to these observed during the sixteenth and seventeenth centuries. Several severe drought episodes occur during the last few decades, albeit less severe than the worst period of drought of the 1540–1670 period. However, the reconstruction shows a trend of decreasing PDSI values over the last few decades, especially in western part of the Mediterranean basin, linked to a trend of increasing temperatures. The continuation of this

warming trend, as shown under future climate scenarios (IPCC 2001; Stott et al. 2004), is likely to result in prolonged and extreme drought conditions over the entire Mediterranean basin. This trend toward increasing periods of drought, coupled with human impact on soil conditions in the southern Mediterranean will have important agricultural and socio-economic consequences for this region, and needs to be taken into account in land management schemes.

Acknowledgments This research has been supported by the European Environment and Sustainable Development programme, project SOAP (EVK2-CT-2002-00160). It is also a contribution to the project ESCARSEL, funded by the French ANR ‘Vulnérabilité: milieux et climat’. The authors wish to thank C. Urbinati (University of Padova), R Motta (University of Torino), E. Gutierrez (University of Barcelona) and JL Edouard (IMEP- University of Marseille) who give us their agreement for the use of unpublished chronologies in our studies. Numerous comments done by the reviewers have helped to significantly increase the paper quality.

7 Appendix: the reconstruction method

Compared to the majority of palaeoclimatological proxies, dendroclimatology has an advantage in having annual time-series for calibrating the relationships between climate and proxies. The relatively low time resolution of other proxies means that variability in time must be replaced by variability in space and a training set must be collected from a wide variety of locations. For these proxies, the modern analogue technique (MAT) has become the leading approach after Hutson (1980), Prell (1985) and Guiot et al (1985), because the method avoids spurious extrapolations and does not affect significantly the reconstructed variance. This is crucial when we are interested in large climatic changes such as glacial-interglacial fluctuations.

For a given past assemblage, the MAT is based on a search for the most similar assemblages among a collection of modern samples. An appropriate distance measure is required in order to evaluate the degree of analogy between past and modern samples. When the method is applied to tree-ring data (Guiot et al. 2005), the assemblages are replaced by annual vectors of proxies, and the objective is to fill missing data in the proxy matrix by using the most similar vectors containing sufficient data. It is possible to use a variety of distance measures, but the Euclidian distance is certainly the most practical here:

$$d_{ts}^2 = \frac{1}{m_{ts}} \sum_{k=1}^{m_{ts}} (p_{tk} - p_{sk})^2 \quad (3)$$

where m_{ts} is the number of proxies simultaneously available for year t (with missing data) and potentially analogue year s , p_{tk} (resp. p_{sk}) is the value of proxy k for year t (resp. year s), d_{ij}^2 is the mean squared Euclidian distance between years t and s . Each proxy series is first standardized so that it ranges between 0 and 1.

The smaller the distance, the greater is the degree of analogy between the two years. Thus, for each proxy series k and year t , we look for analogue years in the other proxy series. A subset of these years is then selected; corresponding to a small number of samples with existing data for proxy series k and the estimated value \hat{p}_{tk} is then

obtained as a weighted average of the same proxy series at the analogous years. As the estimate is an average of a subset from the same statistical population, there is a slight bias in the estimation of its variance. This non-linear approach can be compared to the expectation maximization algorithm proposed by Schneider (2001).

After infilling of the missing proxies, the relationship between instrumental climate series and proxies is calibrated by a non-linear technique (the artificial neural network, ANN) for the period for which climatic data are available. This technique has been largely applied in dendroclimatology (Guiot and Tessier 1997; Woodhouse 1999; D’odorico et al. 2000; Carrer and Urbinati 2001; Ni et al. 2002). We used the feedforward network trained with the backpropagation learning algorithm and validated by a bootstrap technique (Guiot et al. 2005). ANN does not give systematically better results than linear regression, but, when it is carefully applied (avoiding overfitting), it is never worse (Racca et al. 2001). It is better when there are strong non-linearities in the relationship.

References

- Akkemik U, Aras A (2005) Reconstruction (1689–1994 AD) of April–August precipitation in the southern part of central Turkey. *Int J Climatol* 25:537
- Akkemik U, Dag deviren N, Aras A (2005) A preliminary reconstruction (A.D. 1635–2000) of spring precipitation using oak tree-rings in the western Black Sea region of Turkey. *Int J Biomet* 49:297. doi: 10.1007/s00484-004-0249-8
- Akkemik U, D’Arrigo R, Cherubini P, Kose N, Jacoby GC (2007) Tree-rings reconstructions of precipitation and streamflow for north-western Turkey. *Int J Climatol*. doi:10.1002/joc.1522
- Barriendos M (1997) Climatic variations in the Iberian Peninsula during the late Maunder minimum (AD 1675–1715): an analysis of data from rogation ceremonies. *Holocene* 7:105–111
- Barriendos M, Llasat MC (2003) The case of the ‘Malda’ anomaly in the western Mediterranean basin (AD 1760–1800): an example of a strong climatic variability. *Clim Change* 61:191–216
- Barriendos M, Rodrigo FS (2005) Seasonal rainfall variability in the Iberian Peninsula from the 16th century: preliminary results from historical documentary sources. *Geophys Res Abstracts* 7
- Bradley RS (1999) Climatic variability in sixteenth-century Europe and its social dimension—Preface. *Clim Change* 43(1):1–2
- Bradley RS, Jones PD (1993) ‘Little Ice Age’ summer temperature variations: their nature and relevance to recent global warming trends. *Holocene* 3:387–396
- Brazdil R, Pfister C, Wanner H, Von Storch H, Luterbacher J (2005) Historical climatology in Europe—the state of the art. *Clim Change* 70:363–430
- Brewer S, Alleaume S, Guiot J, Nicault A (2006) Historical droughts in Mediterranean regions during the last 500 years: a data/model approach. *Clim Past Discuss* 2:771–800
- Briffa KR (1992) Increasing productivity of “natural growth” conifers in Europe over the last century. In: Bartholin TS, Berglund BE, Eckstein D, Scheiwnguber FH (eds) *Tree rings and environment*. Ystad, Sweden, pp 64–71

- Briffa KR (2000) Annual climate variability in the Holocene: interpreting the message of ancient trees. *Quat Sci Rev* 19(1–5):87–105
- Briffa KR, Jones PD, Schweingruber FH, Osborn TJ (1998) Influence of volcanic eruptions on Northern Hemisphere summer temperatures over 600 years. *Nature* 393:450
- Briffa KR, Osborn TJ, Schweingruber FH, Jones PD, Shiyatov SG, Vaganov EA (2001) Low-frequency temperature variations from a northern tree-ring density network. *J Geophys Res* 106:2929
- Briffa KR, Osborn TJ, Schweingruber FH, Jones PD, Shiyatov SG, Vaganov EA (2002) Tree-ring width and density data around the Northern Hemisphere: part 2, spatio-temporal variability and associated climate patterns. *Holocene* 12:759
- Briffa KR, Osborn TJ, Schweingruber FH (2004) Large-scale temperature inferences from tree-rings: a review. *Global Planet Change* 40:11
- Büntgen U, Esper J, Frank DC, Nicolussi K, Schmidhalter M (2005) A 1052-year tree-ring proxy for Alpine summer temperatures. *Clim Dyn* 25:141–153
- Burger G, Fast I, Cubasch U (2006) Climate reconstruction by regression—32 variations on a theme. *Tellus* 58A 2:227–235
- Carrer M, Urbinati C (2001) Spatial analysis of structural and tree-ring related parameters in a timberline forest in the Italian Alps. *J Veg Sci* 12:645–652
- Casty C, Wanner H, Luterbacher J, Esper J, Böhm RB (2005) Temperature and precipitation variability in the European Alps since 1500. *Int J Climatol* 25:1855–1880
- Cook ER, Jacoby GC (1977) Tree-ring–drought relationships in the Hudson valley, New York. *Science* 198:399–401
- Cook ER, Klaback MA, Jacoby GC (1988) The 1986 drought in the southeastern United States: How rare an event was it? *J Geophys Res* 93:14257–14260
- Cook ER, Briffa K, Shiyatov S, Mazepa V (1990) Tree-ring standardization and growth-trend estimation. In: Cook ER, Kairiukstis LA (eds) *Methods of dendrochronology, applications in environmental sciences*. Kluwer, Dordrecht, pp 104–122
- Cook ER, Stahle DW, Cleaveland MK (1992) Dendroclimatic evidence from eastern North America. In: Bradley RS, Jones PD (eds) *Climate since AD 1500*. Routledge, pp 331–348
- Cook ER, Briffa KR, Jones PD (1994) Spatial regression methods in dendroclimatology—a review and comparison of 2 techniques. *Int J Clim* 14(4):379–402
- Cook ER, Briffa KR, Meko DM, Graybill DA, Funkhouser G (1995) The ‘segment length curse’ in long tree-ring chronology development for palaeoclimatic studies. *Holocene* 5:229–237
- Cook ER, Meko DM, Stahle DW, Cleaveland MK (1999) Drought reconstructions for the continental United States. *J Clim* 12:1145–1162
- Cook ER, Woodhouse CA, Eakin CM, Meko DM, Stahle DW (2004) Long-term aridity changes in the western United States. *Science* 306:1015–1018. doi:10.1126/science.1102586
- Creus J, Beorlegui M, Fernández Cancio A (1995) Reconstrucciones climáticas en Galicia durante las últimas centurias. Estudio dendrocronológico, Xunta de Galicia, Serie monografías, 5, Jaca
- Crowley TJ, Lowery TS (2000) How warm was the medieval warm period? A comment on ‘Man-made *versus* natural climate change’. *Ambio* 39:51–54
- Cullen HM, deMenocal PB (2000) North Atlantic influence on Tigris–Euphrates streamflow. *Int J Climatol* 20:853–863
- Cullen HM, Kaplan A, Arkin PA, deMenocal PB (2002) Impact of the North Atlantic Oscillation on Middle Eastern climate and streamflow. *Clim Change* 55:315
- Dai A, Trenberth KE, Qian T (2004) A global data set of Palmer drought severity index for 1870–2002: relationships with soil moisture and effects of surface warming. *J Hydrometeorol* 5(6):1117–1130
- D’Arrigo RD, Cullen HM (2001) A 350-year (AD 1628–1980) reconstruction of Turkish precipitation. *Dendrochronologia* 19:167–177
- D’Arrigo R, Wilson R, Palmer J, Krusic P, Curtis A, Sakulich J, Bijaksana S, Zulaikah S, La Ode N (2006a) Monsoon drought over Java, Indonesia during the past two centuries. *Geophys Res Lett* 33:L04709. doi:10.1029/2005GL025465
- D’Arrigo RD, Wilson R, Jacoby G (2006b) On the long-term context for late 20th century warming. *J Geophys Res* 111:D03103. doi:10.1029/2005JD006352
- Diodato N (2007) Climatic fluctuations in southern Italy since the 17th century: reconstruction with precipitation records at Benevento. *Clim Change* 80:411–431
- D’odorico P, Revelli R, Ridolfi L (2000) On the use of neural networks for dendroclimatic reconstructions. *Geophys Res Lett* 27:791–794
- Dunkeloh A, Jacobeit J (2003) Circulation dynamics of mediterranean precipitation variability 1948–98. *Int J Climatol* 23:1843–1866
- Efron B (1979) Bootstrap methods: another look at the jackknife. *Ann Stat* 7:1–26
- Esper J, Cook ER, Schweingruber FH (2002) Low frequency signals in long tree-ring chronologies for reconstructing past temperature variability. *Science* 295:2250–2253
- Esper J, Frank DC, Wilson RJS (2004) Climate reconstructions—low frequency ambition and high frequency ratification. *EOS* 85:113–120
- Esper J, Wilson RJS, Frank DC, Moberg A, Wanner H, Luterbacher J (2005) Climate: past ranges and future changes. *Quat Sci Rev* 24:2164–2166
- Esper J, Frank DC, Buntgen U, Verstege A, Luterbacher J, Xoplaki E (2007) Long term drought severity variations in Morocco. *Geophys Res Lett* 34:L17702. doi:10.1029/2007GI030844
- Fernandez J, Saenz J, Zorita E (2003) Analysis of wintertime atmospheric moisture transport and its variability over Southern Europe in the NCEP–Reanalyses. *Clim Res* 23:195–215
- Fritts HC (1976) *Tree rings and climate*. Academic Press, London, 567 p
- Gibelin AL, Deque M (2003) Anthropogenic climate change over the Mediterranean region simulated by a global variable resolution model. *Clim Dyn* 20(4):327–339
- Giorgi F (2006) Climate change hot-spots. *Geophys Res Lett* 33(8):L08707
- Giorgi F, Lionello P (2007) Climate change projections for the Mediterranean region. *Global Planet Change* (in press)
- Glaser R, Brazdil R, Pfister C, Dobrovolny P, Barriendos M, Bokwa A, Camuffo D, Kotyza O, Limanowka D, Racz L, Rodrigo FS (1999) Seasonal temperature and precipitation fluctuations in selected parts of Europe during the sixteenth century. *Clim Change* 43:169
- Gordon C, Cooper C, Senior C, Banks H, Gregory J, Johns T, Mitchell J, Wood R (2000) The simulation of SST, sea ice extents and ocean heat transports in a version of the Hadley Centre coupled model without flux adjustments. *Clim Dyn* 16:147–168
- Greco M, Mirauda D, Squicciarino G, Telesca V (2005) Desertification risk assessment in southern Mediterranean areas. *Adv Geosci* 2:243–247
- Guilbert X (1994) Les crues de la Durance depuis le XIV^{ème} siècle. Fréquence, périodicité et interprétation paléo-climatique. Mémoire de maîtrise de Géographie. Université d’Aix-Marseille I, Aix-en-Provence 350 p
- Guiot J (1985) A method for paleoclimatic reconstruction in palynology based on multivariate time-series analysis. *Géograph Phys Quat* 39:115–125
- Guiot J, Tessier L (1997) Detection of pollution signals in tree-ring series using AR processes and neural networks. In: Rao TS,

- Priestley MB, Lessi O (eds) Applications of time-series analysis in astronomy and meteorology. Chapman & Hall, London, pp 413–426
- Guiot J, Nicault A, Rathgeber C, Edouard JL, Guibal F, Pichard G, Till C (2005) Last-millennium summer-temperature variations in Western Europe based on proxy data. *Holocene* 15(4):1–12
- Hertig E, Jacobeit J (2007) Assessments of Mediterranean precipitations change for the 21st century using statistical downscaling techniques. *Int J Climatol*. doi:10.1002/joc.1597
- Le Houerou HN (1992) Climatic change and desertification. *Impact Sci Soc* 766:183–201
- Huang S (2004) Merging information from different resources for new insights into climate change in the past and future. *Geophys Res Lett* 31. doi:0.1029/2004GL019781
- Hutson WH (1980) The Agulhas current during the late Pleistocene: analysis of modern faunal analogs. *Science* 207:64–66
- IPCC. 2001. Climate change (2001) Impacts, adaptation, and vulnerability. Cambridge University Press, Cambridge
- Jansen E, Overpeck J, Briffa KR, Duplessy J-C, Joos F, Masson-Delmotte V, Olago D, Otto-Bliesner B, Peltier WR, Rahmstorf S, Ramesh R, Raynaud D, Rind D, Solomina O, Villalba R, Zhang D (2007) Palaeoclimate. In: Solomon S, Qin D, Manning M, Chen Z, Marquis M, Averyt KB, Tignor M, Miller HL (eds) Climate change 2007: the physical science basis. Contribution of working group I to the fourth assessment report of the intergovernmental panel on climate change. Cambridge University Press, Cambridge
- Jones PD, Briffa KR, Barnett TP, Tett SFB (1998) High-resolution Palaeoclimatic Records for the Last Millennium: interpretation, integration and comparison with general circulation model control-run temperatures. *Holocene* 8:455–471
- Kutiel H, Maheras P, Guika S (1996a) Circulation indices over the Mediterranean and Europe and their relationship with rainfall conditions across the Mediterranean. *Theor Appl Climatol* 54:125–138
- Kutiel H, Maheras P, Guika S (1996b) Circulation and extreme rainfall conditions in the eastern Mediterranean during the last century. *Int J Climatol* 16:73–92
- Küttel M, Luterbacher J, Zorita E, Xoplaki E, Riedwyl N, Wanner H (2007) Testing a European winter surface temperature reconstruction in a surrogate climate. *Geophys Res Lett* (in press)
- Legutke S, Voss R (1999) ECHO-G, the Hamburg atmosphere-ocean coupled circulation model. DKRZ technical report 18, DKRZ, Hamburg
- Li J, Gou X, Cook E, Chen F (2006) Tree-ring based drought reconstruction for the central Tien Shan area, northwest China. *Geophys Res Lett* 33(7):L07715. doi:10.1029/2006GL025803
- Llasat DCM, Rigo T, Barriendos M (2003) The ‘Montserrat-2000’ flash-flood event: A comparison with the floods that have occurred in the northeastern Iberian Peninsula since the 14th century. *Int J Climatol* 23:453–469
- Llasat MC, Barriendos M, Barrera A, Rigo T (2005) Floods in Catalonia (NE Spain) since the 14th century. Climatological and meteorological aspects from historical documentary sources and old instrumental records. *J Hydrol* 313:32–47
- Luterbacher J, Rickli R, Tinguely C, Xoplaki E, Schupbach E, Dietrich D, Husler J, Ambuhl M, Pfister C, Beeli P, Dietrich U, Dannecker A, Davies TD, Jones PD, Slonosky V, Ogilvie AEJ, Maheras P, Kolyva-Machera F, Martin-Vide J, Barriendos M, Alcoforado MJ, Nunes MF, Jonsson T, Glaser R, Jacobeit J, Beck C, Philipp A, Beyer U, Kaas E, Schmith T, Barring L, Jonsson P, Racz L, Wanner H (2000) Monthly mean pressure reconstructions for the Late Maunder Minimum period (AD 1675–1715). *Int J Climatol* 20:1049–1066
- Luterbacher J, Rickli R, Xoplaki E, Tinguely C, Beck C, Pfister C, Wanner H (2001) The Late Maunder Minimum (1675–1715)—a key period for studying climatic variability and decadal scale climate change in Europe. *Clim Change* 49:441–462
- Luterbacher J, Xoplaki E, Dietrich D, Jones PD, Davies TD, Portis D, Gonzales-Rouco JF, von Storch H, Gyalistras D, Casty C, Wanner H (2002) Extending North Atlantic Oscillation reconstructions back to 1500. *Atmos Sci Lett* 2:114–124
- Luterbacher J, Dietrich D, Xoplaki E, Grosjean M, Wanner H (2004) European seasonal and annual temperature variability, trends and extremes since 1500. *Science* 303:1499–1503
- Luterbacher J, 48 coauthors (2006) Mediterranean climate variability over the last centuries: A review. In: Lionello P, Malanotte-Rizzoli P, Boscolo R (eds) The Mediterranean Climate: an overview of the main characteristics and issues. Elsevier, Amsterdam, pp 27–148
- Mann ME, Bradley RS, Hughes MK (1998) Global-scale temperature patterns and climate forcing over the past six centuries. *Nature* 392:779–787
- Mann ME, Bradley RS, Hughes MK (1999) Northern Hemisphere temperatures during the past millennium: inferences, uncertainties, and limitations. *Geophys Res Lett* 26:759–762
- Mann ME, Rutherford S, Wahl E, Ammann C (2005) Testing the fidelity of methods used in proxy-based reconstructions of past climate. *J Clim* 18:4097–4107
- Meko DM, Cook ER, Stahle DW, Stockton CW, Hughes MK (1993) Spatial patterns of tree-growth anomalies in the United States and southeastern Canada. *J Clim* 6:1773–1786
- Meehl GA, Tebaldi C (2004) More intense, more frequent, and longer lasting heat waves in the 21st century. *Science* 305(5686):994–997
- Melvin TM (2004) Historical growth rates and changing climatic sensitivity of boreal conifers. PhD Thesis. Climate Research Unit, School of environmental science, University of East Anglia, 271p
- Meko DM (1997) Dendroclimatic reconstruction with time varying subsets of tree indices. *J Climate* 10:687–696
- Mika JM, Horvath SZ, Makra L, Dunkel Z (2004) The Palmer drought severity index (PDSI) as an indicator of soil moisture. *Phys Chem Earth* 30:223–230
- Mitchell TD, Carter TR, Jones PD, Hilmu M, New M (2004) A comprehensive set of high-resolution grids of monthly climate for Europe and the globe: the observed records (1901–2000) and 16 scenarios (2001–2100). Tyndall Centre for Climate Change Research, working paper 55:25p
- Moberg AD, Sonechkin M, Holmgren K, Datsenko NM, Karlen W (2005) Highly variable Northern Hemisphere temperatures reconstructed from low- and high-resolution proxy data. *Nature* 433:613–617
- Ni F, Cavazos T, Hughes MK, Combrie A, Funkhouser G (2002) Cool-season precipitation in the Southwestern USA since AD 1000: comparison of linear and non linear techniques for reconstruction. *Int J Climatol* 22:1645–1662
- Nicault A, Guiot J, Brewer S, et Edouard JL (2008) Preserving long-term climatic changes in standardisation of tree-ring series by the Adaptive Regional Growth Curve (ARGC). *Dendrochronologia*
- Osborn TJ, Briffa KR (2006) The spatial extent of 20th century warmth in the context of the last 1200 years. *Science* 311:841–844
- Overpeck J, Hughen K, Hardy D, Bradley RS, Case R, Douglas M, Finney B, Gajewski K, Jacoby K, Jennings A, Lamoureux S, Lasca A, Moore GMJ, Retelle M, Smith S, Wolfe A, Zielinski G (1997) Arctic environmental change of the last four centuries. *Science* 278:1251–1256
- Palmer WC (1965) Meteorological drought. US Weather Bureau. Research paper n 45, Washington DC, 58 p

- Pauling A, Luterbacher J, Casty C, Wanner H (2006) Five hundred years of gridded high-resolution precipitation reconstructions over Europe and the connection to large-scale circulation. *Clim Dyn* 26:387–405
- Pfister C, Brazdil R (1999) Climatic variability in sixteenth-century Europe and its social dimension: a synthesis. *Clim Change* 43:5
- Piervitali E, Colacino M (2001) Evidence of drought in western Sicily during the period 1565–1915 from liturgical offices. *Clim Change* 49:225
- Prell WL (1985) The stability of low-latitude sea-surface temperatures, an evaluation of the CLIMAP reconstruction with emphasis on the positive SST anomalies. Rep TR025, US Dept of Energy, Washington
- Pollack HN, Smerdon JE (2004) Borehole climate reconstructions: spatial structure and hemispheric averages. *J Geophys Res*, 109. doi:10.1029/2003JD004163
- Purgstall BJVH (1983) Ottoman state history, vol 1–7. Translator: Vecdi Burun, Uc, dal Publishing, Istanbul (in Turkish)
- Racca JMJ, Philibert A, Racca R, Prairie YT (2001) A comparison between diatom-based pH inference models using artificial neural networks (ANN), weighted averaging (WA) and weighted averaging partial least squares (WA-PLS) regressions. *J Paleolimnol* 26:411–422
- Rambal S, Debussche G (1995) Water balance of Mediterranean ecosystems under a changing climate. In: Moreno J, Oechel WC (eds) Anticipated effects of a changing global environment on Mediterranean-type ecosystems, Ecological Studies 117. Springer, New York, pp 386–407
- Rathgeber C, Guiot J, Roche P, Tessier L (1999) Augmentation de productivité du chêne pubescent en région méditerranéenne française. *Ann Sci For* 56:211–219
- Rodrigo FS, Esteban-Parra MJ, Pozo-Vazquez D, Castro-Diez Y (1999) A 500-year precipitation record in Southern Spain. *Int J Climatol* 19:1233–1253
- Rodrigo FS, Esteban-Parra MJ, Pozo-Vazquez D, Castro-Diez Y (2000) Rainfall variability in Southern Spain on decadal to centennial time scales. *Int J Climatol* 20:721
- Rodrigo FS, Pozo-Vazquez D, Esteban-Parra MJ, Castro-Diez Y (2001) A reconstruction of the winter North Atlantic Oscillation Index back to AD 1501 using documentary data in southern Spain. *J Geophys Res* 106:14805–14818
- Rumelhart DE, Hinton GE, Williams RJ (1986) Learning representations by back-propagating errors. *Nature* 323:533–536
- Rutherford S, Mann ME, Osborn TJ, Bradley RS, Briffa KR, Hughes MK, Jones PD (2005) Proxy-based Northern Hemisphere surface temperature reconstructions: sensitivity to method, predictor network, target season and target domain. *J Clim* 18:2308–2329
- Saz MA (2004) Temperaturas y precipitaciones en la mitad norte de España desde el siglo XV. Estudio dendroclimático. Consejo de Protección de la Naturaleza. Diputación General de Aragón, Zaragoza, p 294
- Schneider T (2001) Analysis of incomplete climate data: estimation of mean values and covariance matrices and imputation of missing values. *J Clim* 14:853–871
- Stahle DW, Cleaveland MK (1988) Texas drought history reconstructed and analyzed from 1698–1980. *J Clim* 1:59–74
- Stahle DW, Hehr JG (1985) A 450-year drought reconstruction for Arkansas, United States. *Nature* 316:530–532
- Stockton CW, Meko DM (1983) Drought recurrence in the Great Plains as reconstructed from long-term tree-ring records. *J Clim Appl Meteor* 22:17–29
- Stott PA, Stone DA, Allen MR (2004) Human contribution to the European heatwave of 2003. *Nature* 432:610–614
- Till C, Guiot J (1988) Reconstruction of precipitation in Morocco since 1100 A.D. based on *Cedrus atlantica* tree-ring widths. *Quat Res* 33:337–351
- Touchan R, Meko D, Hughes MK (1999) A 396-year reconstruction of precipitation in southern Jordan. *J Am Water Resour As* 35(1):49–59
- Touchan R, Garfin GM, Meko DM, Funkhouser G, Erkan N, Hughes MK, Wallin BS (2003) Preliminary reconstructions of spring precipitation in southwestern Turkey from tree-ring width. *Int J Climatol* 23:157
- Touchan R, Xoplaki E, Funkhouser G, Luterbacher J, Hughes MK, Erkan N, Akkemik U, Stephan J (2005) Reconstructions of spring/summer precipitation for the Eastern Mediterranean from tree-ring widths and its connection to large-scale atmospheric circulation. *Clim Dyn* 25:75–98
- Van der Schrier G, Briffa KR, Jones PD, Osborn TJ (2006) Summer moisture variability across Europe. *J Clim* 19:2818–2834
- Van der Schrier G, Efthymiadis D, Briffa KR, Jones PD (2007) European Alpine moisture variability for 1800–2003. *Int J Climatol* 24:415–427
- Vinther BM, Andersen KK, Hansen AW, Schmith T, Jones PD (2003) Improving the Gibraltar/Reykjavik NAO Index. *Geophys Res Lett* 30:2222. doi:10.1029/2003GL018220
- Von Storch H, Zorita E, Jones JM, Dimitriev Y, Gonzalez-Rouco F, Tett SFB (2004) Reconstructing past climate from noisy data. *Science* 306:679–682
- Wells N, Goddard S, Hayes MJ (2004) A Self-calibrating Palmer drought severity index. *J Clim* 17:2335–2351
- Woodhouse CA (1999) Artificial neural networks and dendroclimatic reconstructions: an example from the Front Range, Colorado, USA. *Holocene* 9:521–529
- Xoplaki E (2002) Climate variability over the Mediterranean. PhD Thesis, University of Bern, Switzerland
- Xoplaki E, Maheras P, Luterbacher J (2001) Variability of climate in meridional Balkans during the periods 1675–1715 and 1780–1830 and its impact on human life. *Clim Change* 48:581–615
- Xoplaki E, Gonzalez-Rouco JF, Luterbacher J, Wanner H (2003) Mediterranean summer air temperature variability and its connection to the large-scale atmospheric circulation and SSTs. *Clim Dynam* 20:723–739
- Xoplaki E, Gonzalez-Rouco JF, Luterbacher J, Wanner H (2004) Wet season Mediterranean precipitation variability: influence of large-scale dynamics and trends. *Clim Dyn* 23:63–78
- Xoplaki E, Luterbacher J, Paeth H, Dietrich D, Steiner N, Grosjean M, Wanner H (2005) European spring and autumn temperature, variability and change of extremes over the last half millennium. *Geophys Res Lett* 32:L15713. doi:10.1029/2005GL023424
- Xoplaki E, Luterbacher J, González-Rouco JF (2006) Mediterranean summer temperature and winter precipitation, large-scale dynamics, trends. *Il Nuovo Cimento* 29:45–54
- Yiou P, Nogaj M (2004) Extreme climatic events and weather regimes over the North Atlantic: When and where? *Geophys Res Lett* 31(7):L07202
- Zobler L (1999) Global Soil Types, 1-Degree Grid (Zobler). Data set. Available on-line [<http://www.daac.ornl.gov>] from Oak Ridge National Laboratory Distributed Active Archive Center, Oak Ridge
- Zorita E, Gonzalez-Rouco F, Legutke S (2003) Testing the Mann et al. (1998) approach to paleoclimate reconstructions in the context of a 1000-year control simulation with the ECHO-G coupled climate model. *J Clim* 16:1368–139